Journal of Anthropology and Archaeology
June 2017, Vol. 5, No. 1, pp. 20-38
ISSN 2334-2420 (Print) 2334-2439 (Online)

Published by American Research Institute for Policy Development
DOI: 10.15640/jaa.v5n1a3
URL: https://doi.org/10.15640/jaa.v5n1a3

An Osseous Remain on the Face of the Turin Shroud

G. Lucotte[1] & T. Thomasset[2]

Abstract

Turin Shroud is a well-known Christ relic on which a body image is imprinted. We had access to a sticky-tape that was applied directly to one blood spot of the Face. This sticky-tape contains very numerous microscopic particles, that were studied by optical microscopy and SEM-EDX analysis. One of these particles, named e58, is a bone/cartilage remain; it was intensively studied for its aspect, colour, thickness, surface morphology and ultrastructure, and for its organic and mineral compositions. Presence of such an osseous remain on the Face adds new substantial material (other than red blood cells, skin debris and one hair, already published) to the knowledge of the Man whose body is imprinted on the Turin Shroud.

Keywords: Face ; microscopic particles ; optical microscopy ; osseous remain ; SEM-EDX ; sticky-tape ; Turin Shroud.

Introduction

The Turin Shroud (TS) , a well-known Christ's relic, is an intensively studied object on which a body image is imprinted (e.g. Marion and Lucotte, 2006). The frontal image of the Head (Face and Hair) , notably, is visible with the naked eye. G. Riggi di Numana (Riggi di Numana, 1988) transmitted to one of us (G.L.) a small (1.36 mm high, 614 µm wide) sticky-tape triangle, that is some part of a larger piece he placed directly (during the 1978 official sampling on the TS surface) at one "blood area" of the Face. I (G.L.) have studied this triangle, by optical and electronic microscopy (Lucotte, 2012). More than 1500 particles, greater than or equal to 1 µm, can be observed on its surface. For practical reasons, this surface was subdivided into 19 areas (A to S) containing almost all the particles observed. We have found on the triangle surface portions of textile (mainly linen) fibers (Lucotte, 2015a), pollen grains and spores (Lucotte, 2015b), red blood cells (Lucotte, 2015c), skin debris (Lucotte 2016a) and one hair (Lucotte and Thomasset, 2017).

We describe here the only particle found on the triangle surface that can be assimilated to an osseous remain.

Material and Methods

The e58 particle studied is located in the E area of the triangle. It is ovaloid in form, with dimensions of 10 on 8.2 µm. Optical observations were realized using a photomicroscope Zeiss, model III, 1972 ; the studies in cross-polarized light were realized with the petrographic version of this microscope. Two SEM (Scanning Electron Microscopy) apparatus (both of Environmental types) were used further. The first one (SEM1) is a Philips XL30 instrument ; GSE (Gaseous Secondary Electrons) and BSE (Back Scattered Electrons) are used, the last one to detect heavy elements.

1 Institute of Molecular Anthropology, Paris, France, Gérard Lucotte, Institut d'Anthropologie Moléculaire, 42 rue Monge, 75005 Paris France,
2 Laboratory of Physico-Chemical Analysis, UST of Compiègne, France

Elemental analysis of the particles was achieved by using EDX (Energy Dispersive X-ray spectroscopy), this SEM1 microscope being equipped with a Bruker AXS-EDX (PGT system analysis: Spirit model, of Princeton Gamma Technology). Each elemental analysis is given in the forms of a spectrum, with kiloelectrons / Volts (ke/V) on the abscissa and elemental peak heights in ordinates. Estimating peaks heights, it is possible to realize some semi-quantitative studies. The "in relief" image was realized in BSE, by substracting (A_B) the signals obtained by the two semiconductor captors (A and B) located under the polar piece of the objective. The second apparatus (SEM2) is a FEI model Quanta 250 f FEG (probe model X-flash 6/30) ; both LFD (Large Field Detector) and CBS (Circular Back Scattering) procedures were used. It is with this second apparatus that high-resolution imaging and elemental mapping of the particles were realized. EDX-mapping was obtained (power : 20 kV ; distance : 9.9 mm ; acquisition time : 15 min.) for the main elements : C, O, P, Ca and Pb.

Results and Discussion

Location of e58 in the E area Because of its complexity, area E of the triangle was further subdivided in seven E sub-areas : a, b, c, d, e , f and g (Figure 1). The e58 particle is located in the Ec sub-area, near the right medium corner of this zone.

Figure 1 . A SEM1 1250x photograph (in GSE) of the E area (subdivided in sub-areas a,b,c,d,e,f and g) of the triangle. The red pastille indicates location of the e58 particle ; locations of two other particles (e55 : lead, and e49 : gold), inside the Ec sub-area, are also indicated.

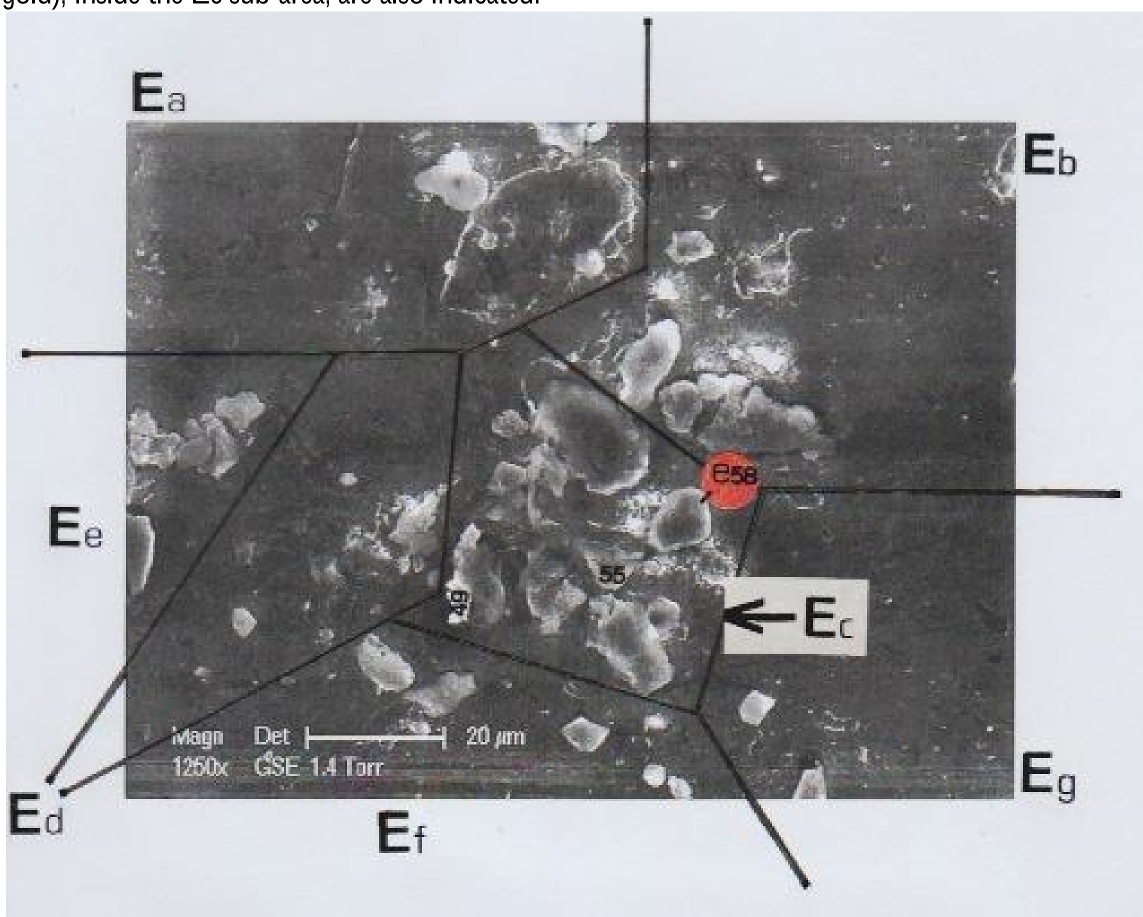

The e58 colour

The optical microscopy view of the E area shows that the e58 colour is yellow-white (Figure 2.1). The e58 particle does not birefract in polarized light (Figure 2.2).Surrounding e58 particles Figure 2. Optical microscopy (inverted) views (1200x) of particles located in area E (f :left border of the triangle) ; the triangle pastilles indicate location of the e58 particle. Above **1**/ coloured view of the particles. Below **2**/the same optical view, but in polarized light. In that view, locations of other particles (F4 : linen fiber number 4 ; e49 : gold ; e50 : two Cyanophycaes ; e54 : calcium carbonate ; e55 : lead ; e57 : mineral covered by plastic ; e58' : hematy ; e64 : organic matter) are also indicated.

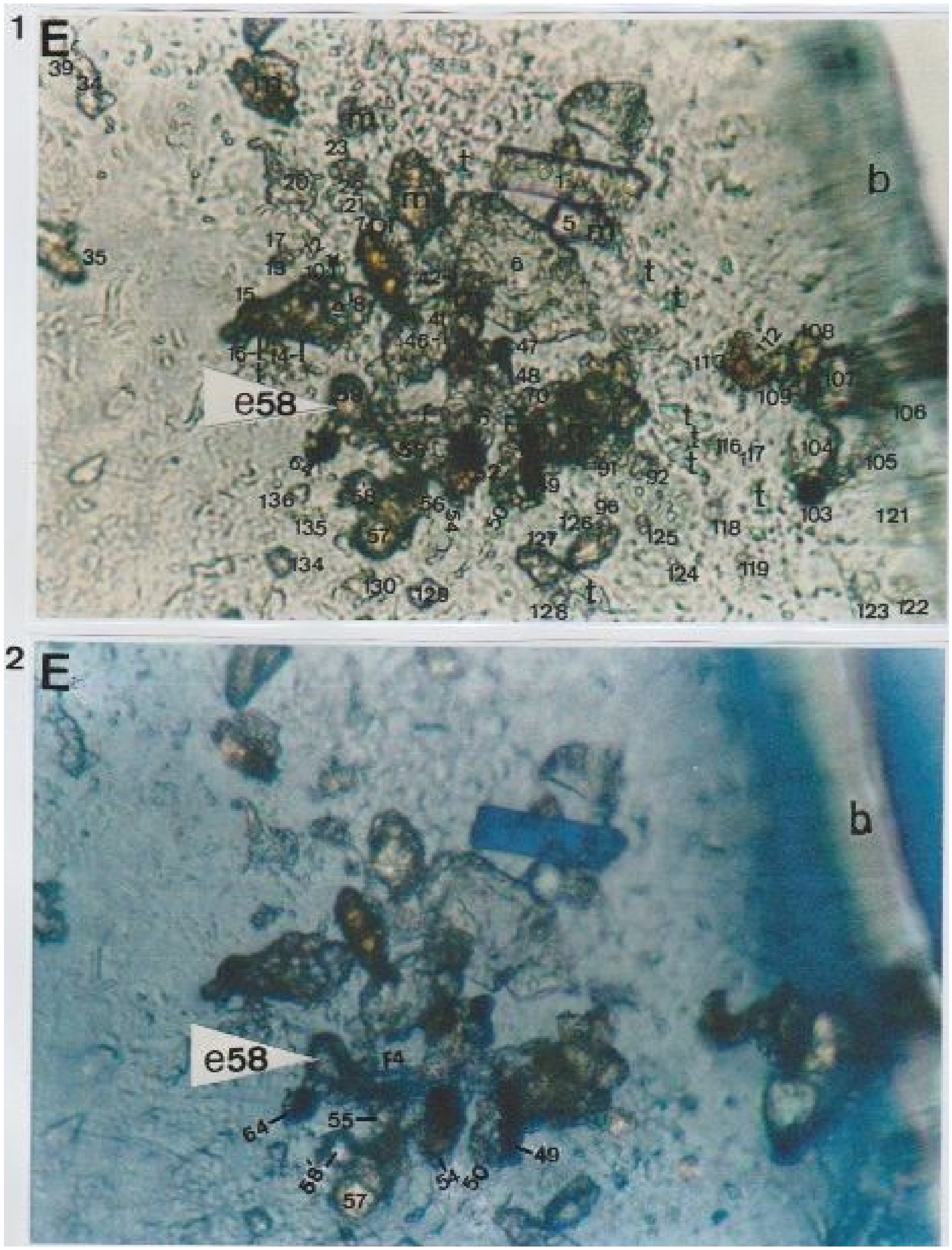

Figure 3. A SEM1 5000x photograph (in GSE) of the Ec sub-area showing e58 and other surrounding particles (enumerated in table 1).

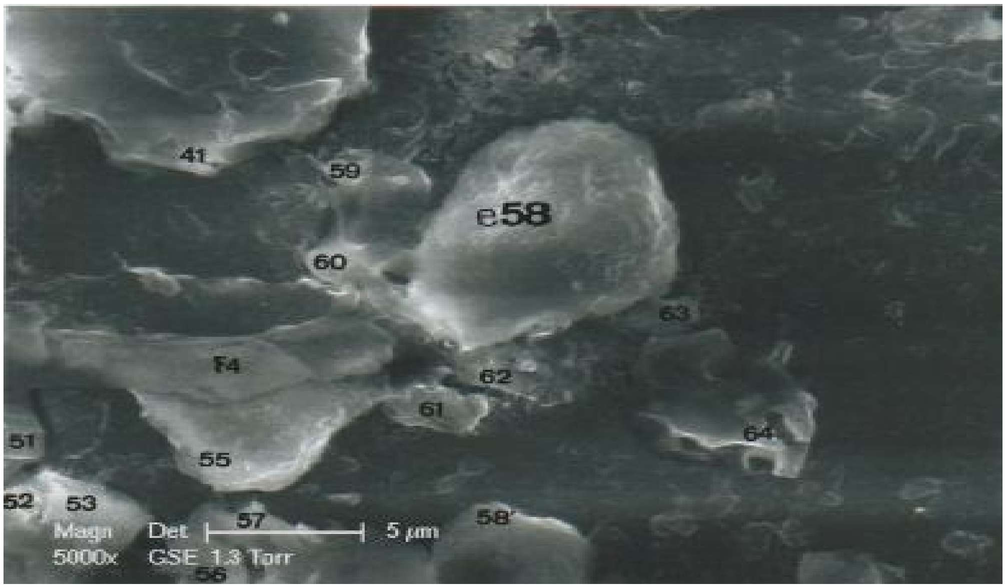

The Figure 3 SEM1 (in GSE) photograph shows the ten particles (e41, F4, e55, e51, e52, e53, e56, e57, e58' and e64) in the Ec sub-area surrounding e58. Table 1 summarizes their characterizations : e41 is the lower part of a mineral of the aluminosilicate type ; e64 is mainly composed of organic matter. F4 is the fourth linen fiber previously characterized. The e55 particle is mainly composed of lead ; e51 is a little black spore, already observed. The particles e52 and e53 are two coupled Dinophycaes (unicellular marine algae) ; e56 and e57 represent the top portions of two plastic lobes covering a relatively big mineral particle ; e58' is a hematy.

Aspect and composition of e58

Table 1. Particles surrounding e58 (In figure 3).

Particles	Characterizations	References
e41	aluminosilicate	
e64	organic matter	
F4	linen fiber number 4	Lucotte, 2015a
e55	lead	
e51	a black spore	Lucotte, 2015b
e52	- two Dinophycaes	
e53		
e56	- two plastics	
e57		
e58'	a hematy	Lucotte, 2015c

The Figure 4 photograph shows a detailed view (10000x) of the e58 particle in GSE ; some micro-ornamentations are visible on the particle surface. The e58 spectrum establishes that it is mainly composed of phosphorus and of calcium (calcium phosphate). We know (e.g. Garcia Garduno et al., 2010) that the main mineral component of bones is a special sort of calcium phosphate named hydroxyapatite (HA).Figure 4. Above : A SEM1 10000x photograph (in GSE) of e58 (the black dot indicates the point where EDX analysis is realized). Below : the EDX spectrum of e58. C : carbon ; O : oxygen ; Si : silicium ; P : phosphorus ; Ca (two peaks) : calcium.

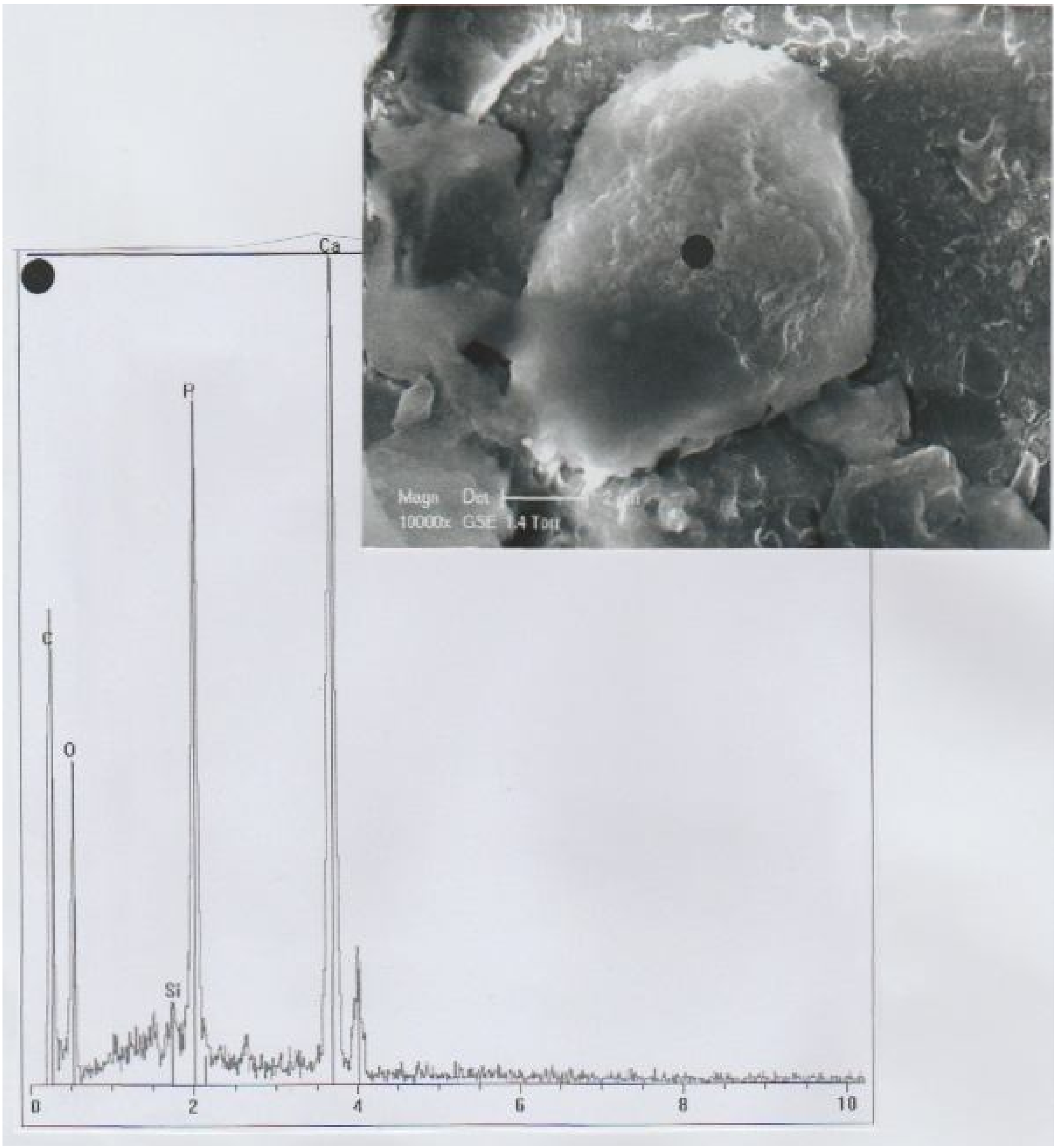
Ca
P
C
O
Si
0
2
4
6
8
10
Magn Det
10000x GSE 1.4 Torr

Figure 5. Two SEM1 photographs (in BSE) of the e58 particle. Above **1/** : 10 000x. Below **2/**12 000x ; D : great (apparent) deposit.

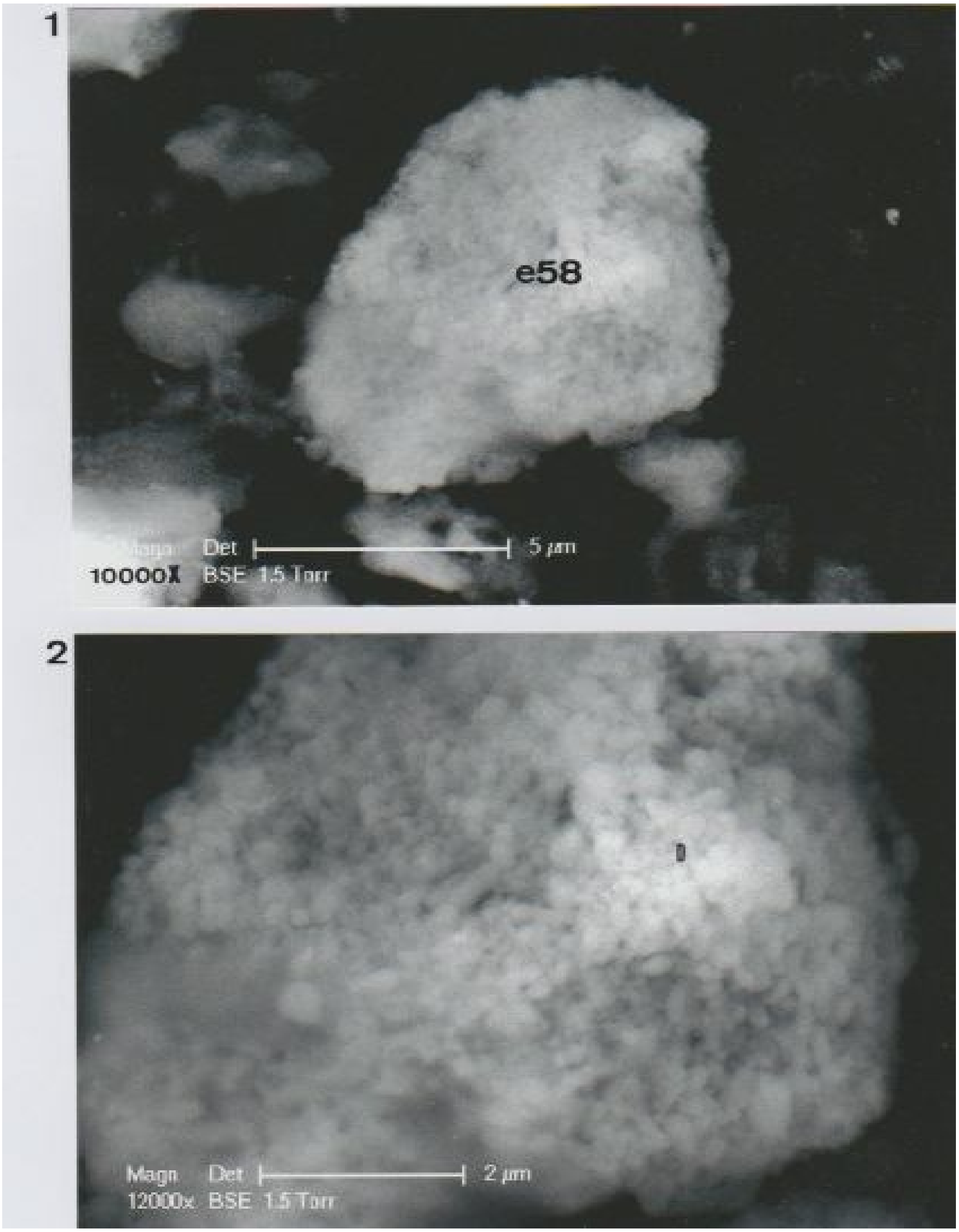

But in the spectrum are also two relatively important peaks of carbon and of oxygen ; that indicates the presence of some amount of organic matter in the sample. Ultrastructure of e58 studied in BSE The two SEM1 photographs of Figures 5.1 and 5.2 show the e58 particle in BSE, at two increasing magnifications. On the magnification of 12000x (Figure 5.2), we can see the particle is entirely formed of fine (100nm-1µm) well delimited micrograins.

These micrograins appear as microstructures that are light (in BSE) to electrons ; they constitute the inorganic (HA) component of the bone. In the D zone of figure 2.2 the BSE signal is lighter again, corresponding to an increased density of the calcium element ; micrograins in this zone are probably quasi-crystals of tricalcium phosphate (TCP).Thickness of e58. On the "in relief" photograph (in BSE) of Figure 6 we can see that the e58 particle had some notable thickness, contrary to other neighbouring particles (including F4) ; the lead (e55) and the gold (e49) particles have also some thickness.

High-resolution SEM2 study of e58

The high-resolution SEM2 6000x photograph (in LFD) of Figure 7 shows some supplementary details of the e58 surface : otherwise that the granular micro-structure previously described, we can distinguish (in the left part of the particle) another aspect of the ornamentation consisting of micro-reliefs orientated longitudinally ; that is the fibrous micro-structure of the particle. The corresponding spectrum1 concerns an elemental EDX-analysis that was realized in the fibrous part of the e58 particle. The more elevated peak of the spectrum matrix is mainly constituted of collagen microfilaments (Catanese et al., 1999). The main mineral elements of the spectrum are calcium and phosphorus. The calculated Ca/P ratio is close to the ideal value of 1.69 for a bone sample (Joschek et al. , 2000). There are small peaks in the spectrum for sodium, magnesium, aluminium, silicium, lead and chlorine, and some traces of iron. Tables 2 gives the normalized composition in mineral elements of the spectrum.

Table 2. Normalized composition (carbon and oxygen excepted) of elements in the spectrum of figure 7.

Elements	Atomic numbers	Rays	Normalized mass (%)
Silicium	14	K-serie	6.78
Calcium	20	K-serie	52.49
Sodium	11	K-serie	2.88
Magnesium	12	K-serie	3.79
Aluminium	13	K-serie	4.44
Phosphorus	15	K-serie	15.56
Lead	82	M-serie	10.31
Chlorine	17	K-serie	0.53
Iron	26	K-serie	3.22
Total			100.00

Sodium, magnesium and silicium are normal minor chemical elements in the bone composition. In the present case the silicium peak is enhanced and there is small abnormal peak of aluminium ; that suggests that there are some deposits of montmorillonite (an ubiquitous clay composed of Si, Al, Mg, Ca and with iron traces) at the e58 surface. Chlorine is not usually present in bones ; but this element constitutes salt (ClNa) with the sodium, and probably the e58 particle surface is also contaminated by this product. Presence of lead in the spectrum (it represents more than 10% of the normalized composition) is highly abnormal. We can explain later this massive metallic contamination. The SEM2 photograph (in LFD) of Figure 8 shows an enlarged view (2400x) of the rectangular area indicated in the figure 7 photograph. We can see that most of the micrograins located in the photograph left-part are lengthened longitudinally : they constitute the "fibrous" part of the area (in opposition to the "granular" part, located at the right).

Figure 6. An in relief SEM1 1500x photograph (in BSE) of e58 and other neighbouring particles (F4, e55 and e49 are indicated).

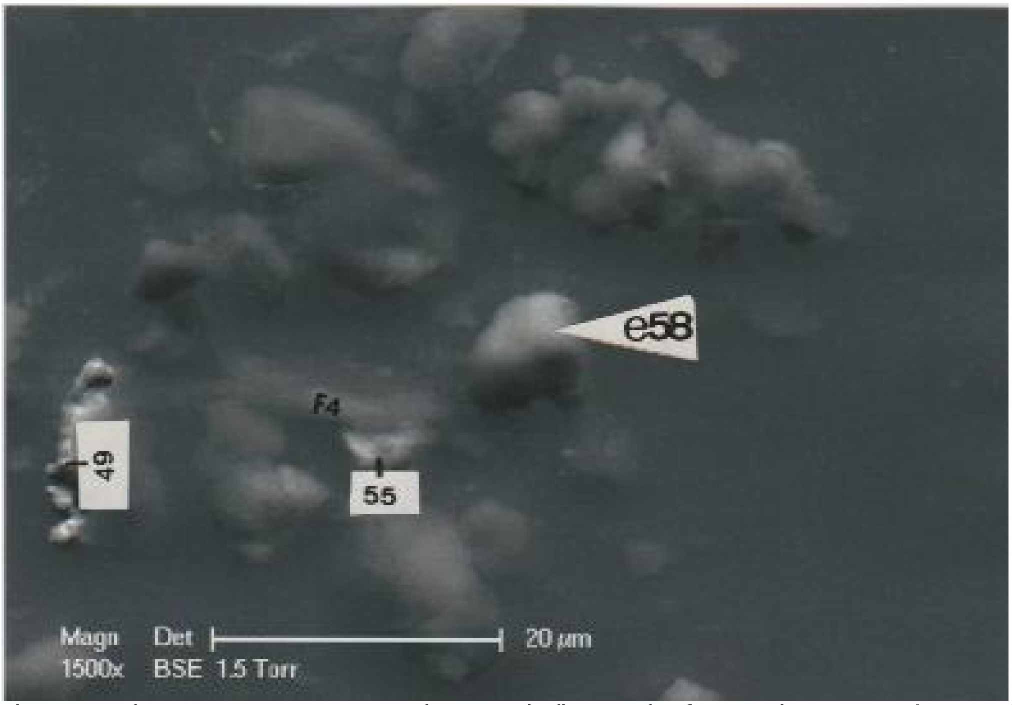

Figure 7. Above : A SEM2 6000x photograph (in LFD) of e58. The rectangular area is enhanced on figure 8 (F : fibrous sub-area ; G : granular sub-area). Below : The EDX spectrum of e58. Fe (three peaks) : iron ; Na : sodium ; Mg : magnesium ; Al : aluminium ; Pb : lead ; Cl : chlorine.

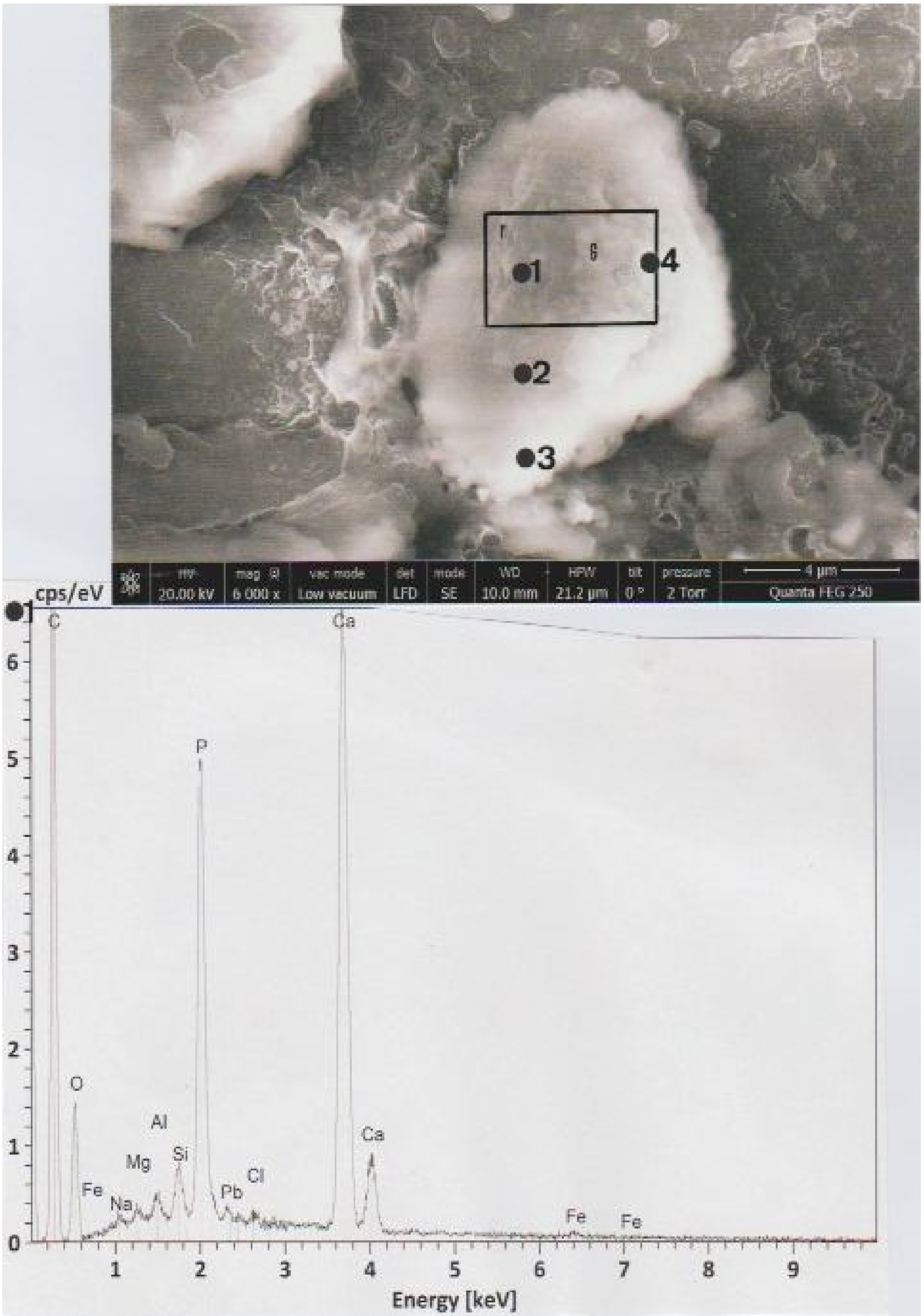
1
2
3
4
mag
vac mode
det
mode
WD
HFW
tilt
pressure
4 µm
20.00 kV
6 000 x
Low vacuum
LFD
SE
10.0 mm
21.2 µm
0 °
2 Torr
Quanta FEG 250
cps/eV
C
Ca
P
O
Al
Mg
Si
Fe
Na
Pb
Cl
Ca
Fe
Fe
0
1
2
3
4
5
6
Energy [keV]

Spectrum 1 of figure 7 shows that this first part, contrary to the granular one showed in the figure 4 corresponding spectrum, is relatively rich in organic matter (mainly the carbon, but oxygen also). This organic phase of the osseous mineral is that of the carbon (and the ordinates gradation of oxygen attains a 1.4 value) ; this indicates the relative riches in organic matter of the fibrous part of the particle.It seems that there is an increase of the organic matter along the vertical axis of the e58 particle (Figure 9) : at the point 2 of the figure 7 photograph, the carbon peak is at the value of 7.2 on the ordinates axis (the phosphorus value is of 2.8 , and the calcium value is of 3.7), when the carbon peak value reaches 9 at the point 3 (the phosphorus value is of 1 and the calcium value is of 1.6). This increase of the organic mass, compared to the relative decrease of the osseous mineral matter, indicates that the e58 inferior basis is mainly constituted of another biological sclerified material (cartilage, tendon , or even flesh) than bone.Concerning now point 4 of the figure 7 photograph (located in the D zone of the figure 8 photograph), the corresponding spectrum in figure 9 shows that calcium (which attains a value of 3) is the main mineral component. It is the reason why we have considered that the D zone is mainly constituted of TCP crystals ; but calcium carbonate , that is a normal-but relatively minor bone component, can also be present here. This e58 peculiar zone shows all the characteristics of a local hyper-hated point (Miculescu et al., 2011).

Figure 8. A SEM2 24000x photograph (in LFD) of the rectangular area of figure 7 (F : fibrous sub-area ; G : granular sub-area ; D : great deposit of confluent G sub-particles).

Figure 9. Spectras of e58 at the 2 (above) , 3 (medium) and 4 (below) points of elemental analysis indicated in the figure 7 photograph.

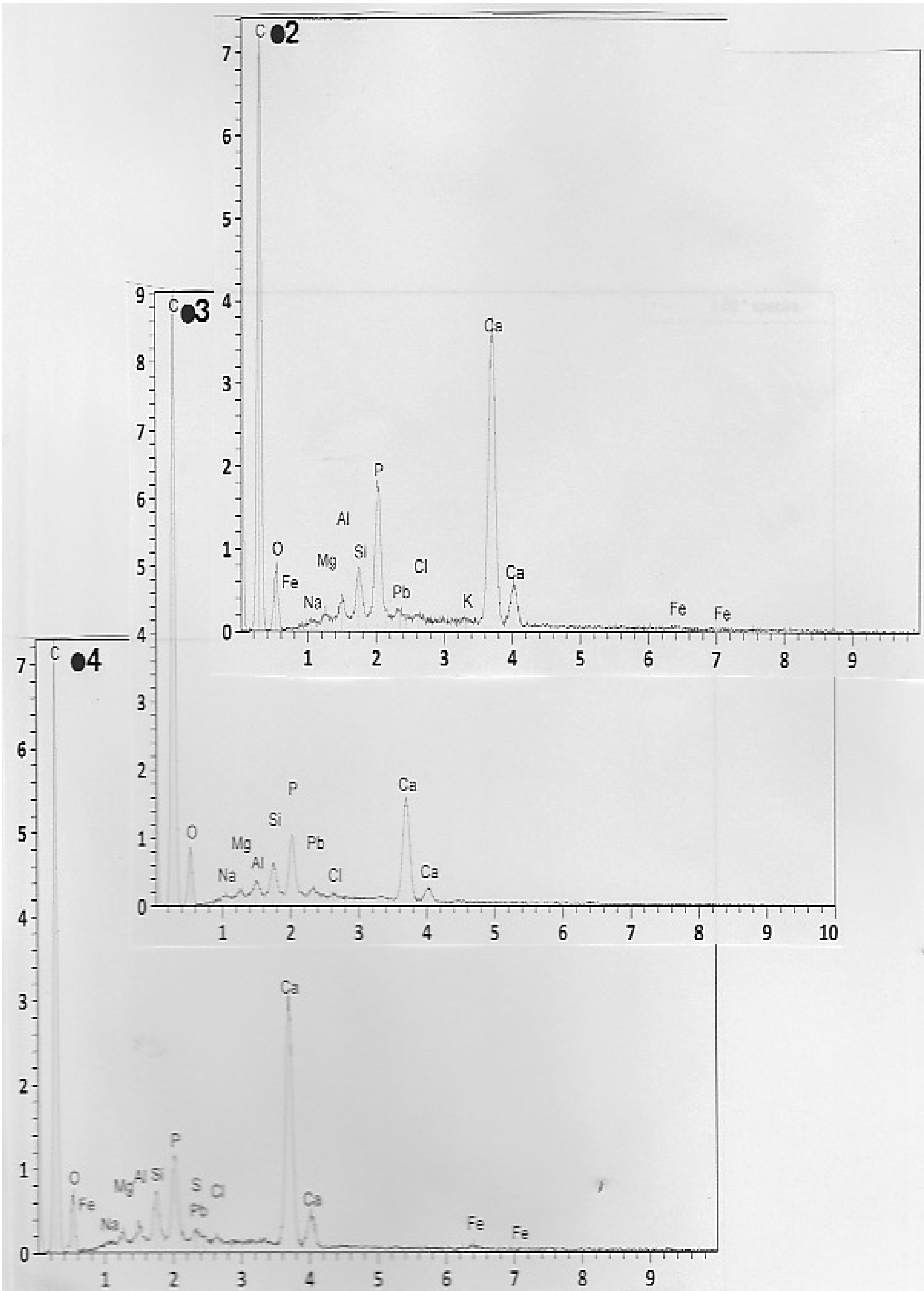

Figure 10. Two SEM2 6000x photographs of the particles nearly surrounding e58. Above **1/** in LFD. Below **2/** in CBS ; particles e55, e59, e60, e61 , e62 , e63 and e64 indicated.

1

2

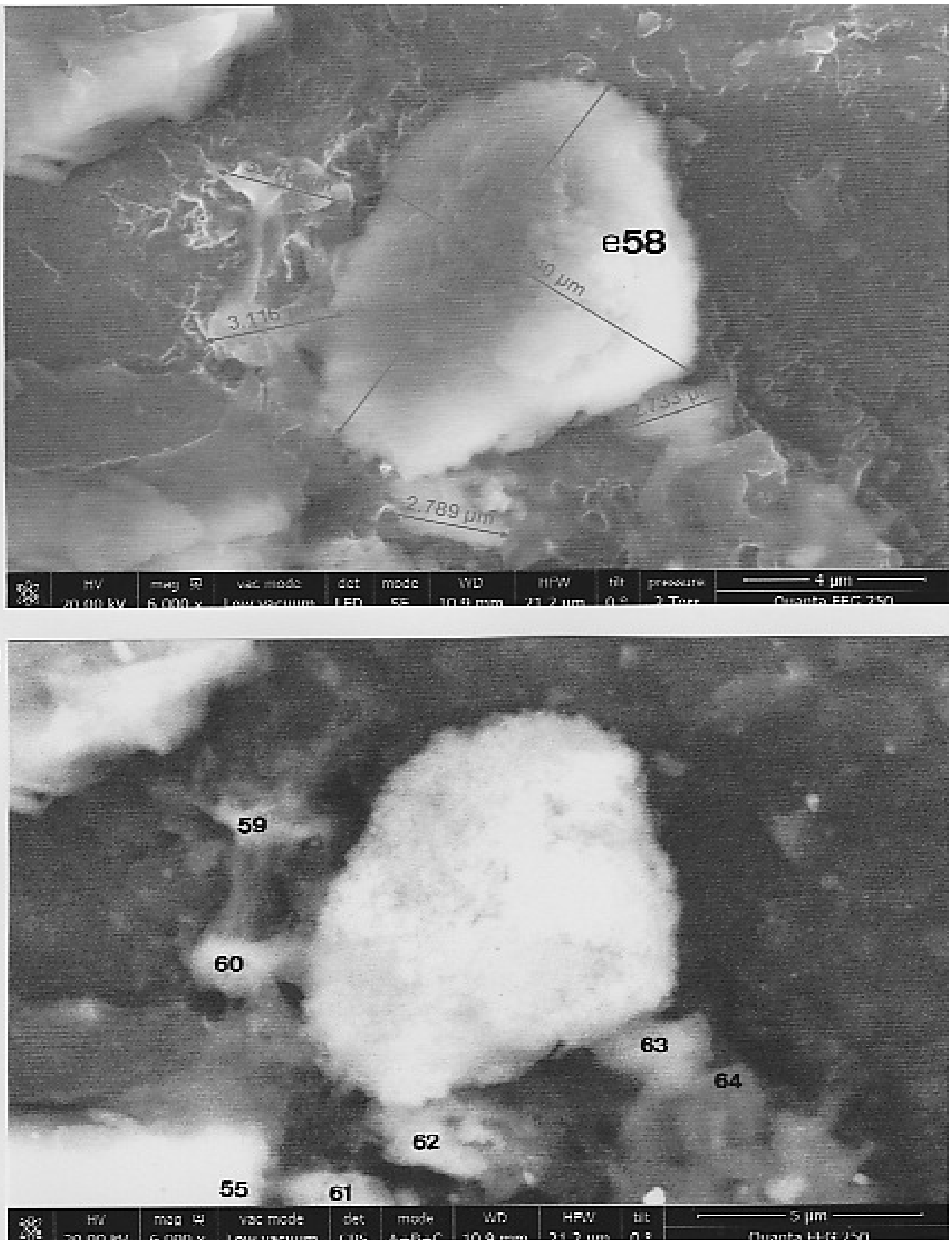

Figure 11. Spectras of particles e63 (above), e62 (medium) and e59-e60 (below) ; the supplementary elements in the third spectrum are copper (Cu : three peaks), cadmium (Cd) and barium (Ba : two peaks).

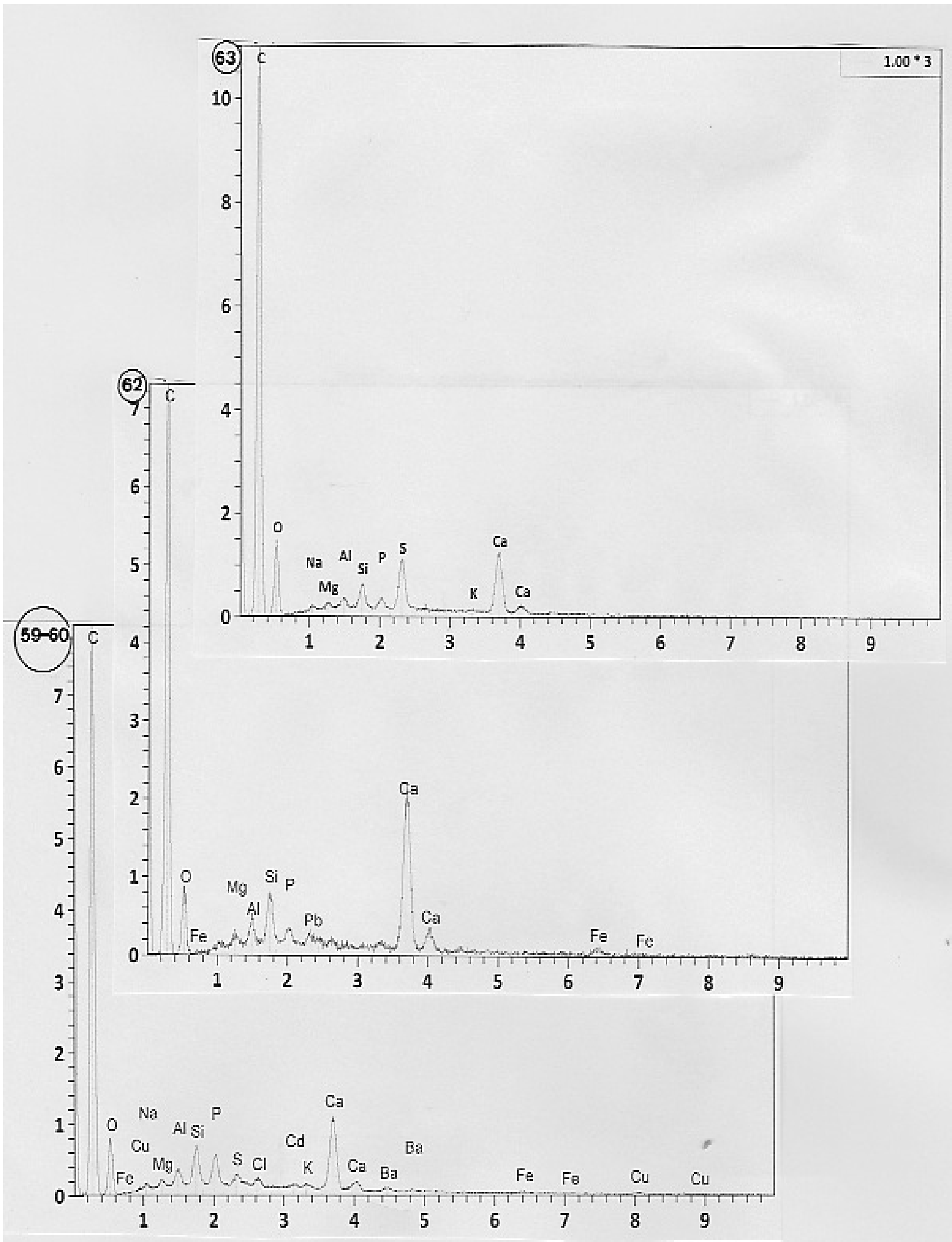

Figure 12. Spectras of particles e61 (above) and e55 (below).

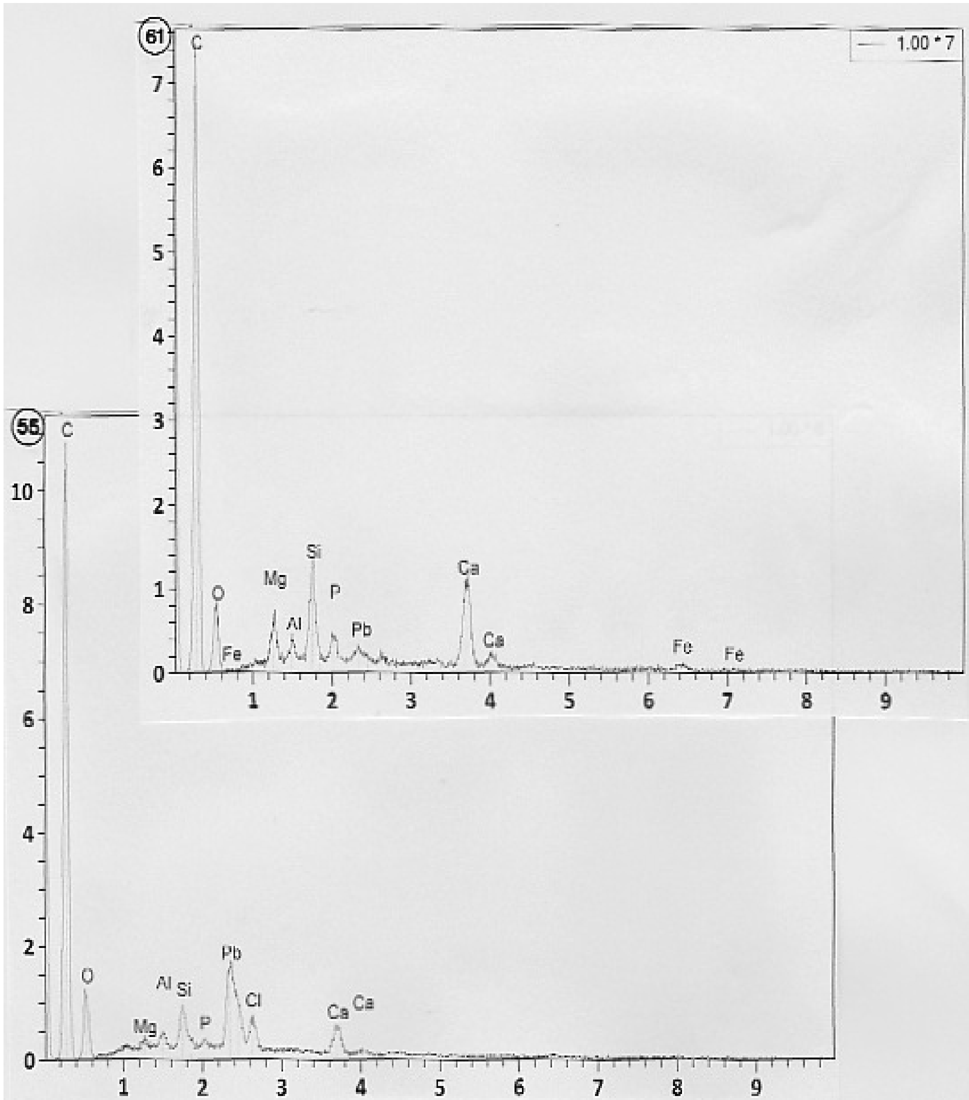

Figure 13. Mapping of elements of e58 and surrounding particles. First row : A SEM2 5000x map (in LFD) showing particles e58, e41, e55, F4, e59, e60, e61, e62, e63 and e64. Second row : maps of carbon (C) and oxygen (O) ; third row : maps of phosphorus (P) and calcium (Ca) ; fourth row : map of lead (Pb).

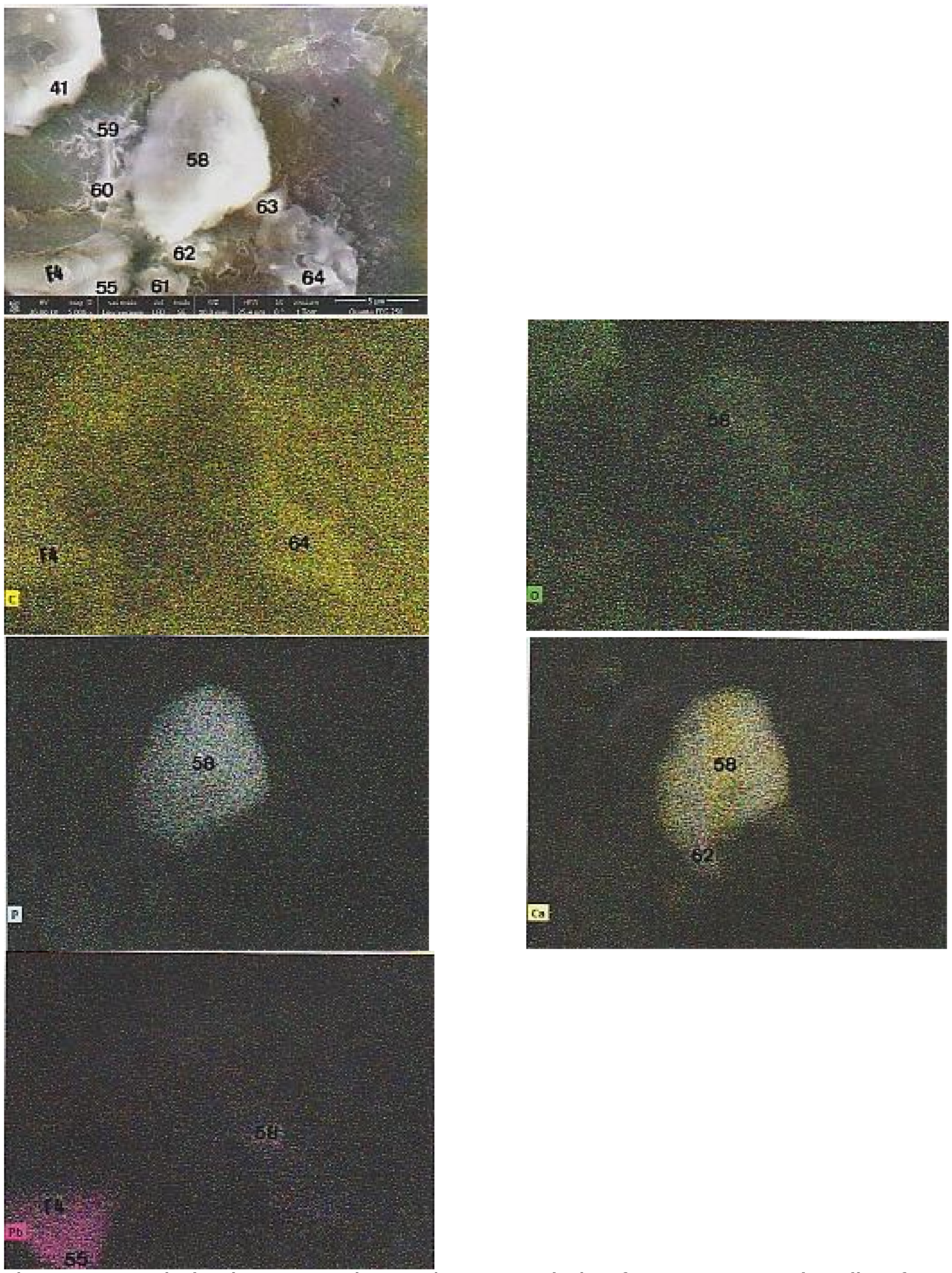

Figure 14. Optical microscopy view and EDX-analysis of an osseous scale relic of Ste Marie-Madeleine. Above **1** / coloured view (15x) of the scale. Below **2**/ EDX spectrum of the scale.

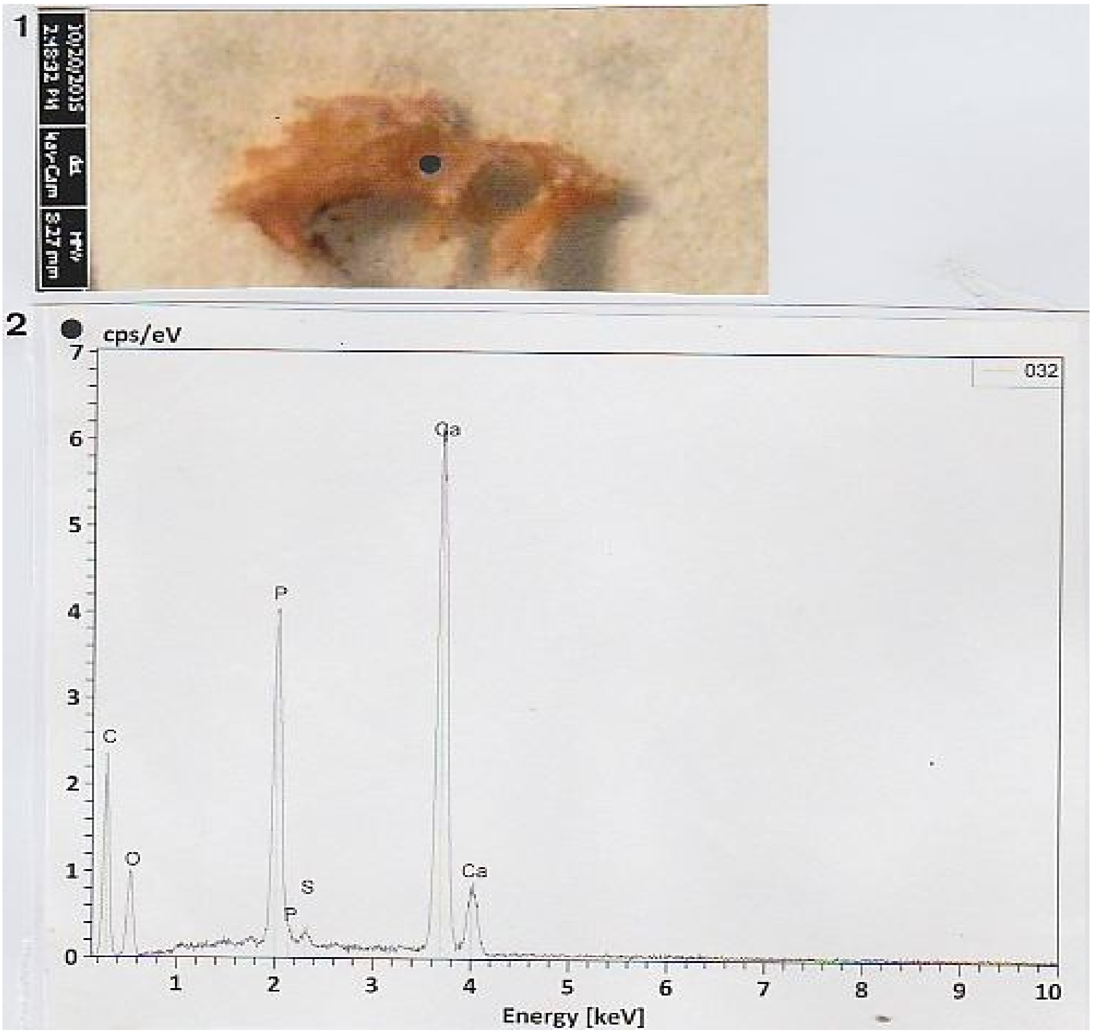

Figure 15. Schematic representation of the bone particle. Circled numbers indicate the different particles : 1 (e58), 2(e59, in red), 3 (e60, in red), 4 (e62) and 5 (e63). The e58 particle is further divided in its three sub-parts : a (the “osseous” sub-part in yellow), b (the “cartilageous” sub-part, in orange) and c (the “heated” subpart, in grey) ; the thin line between the two e58 sub-parts a and b is indicative.

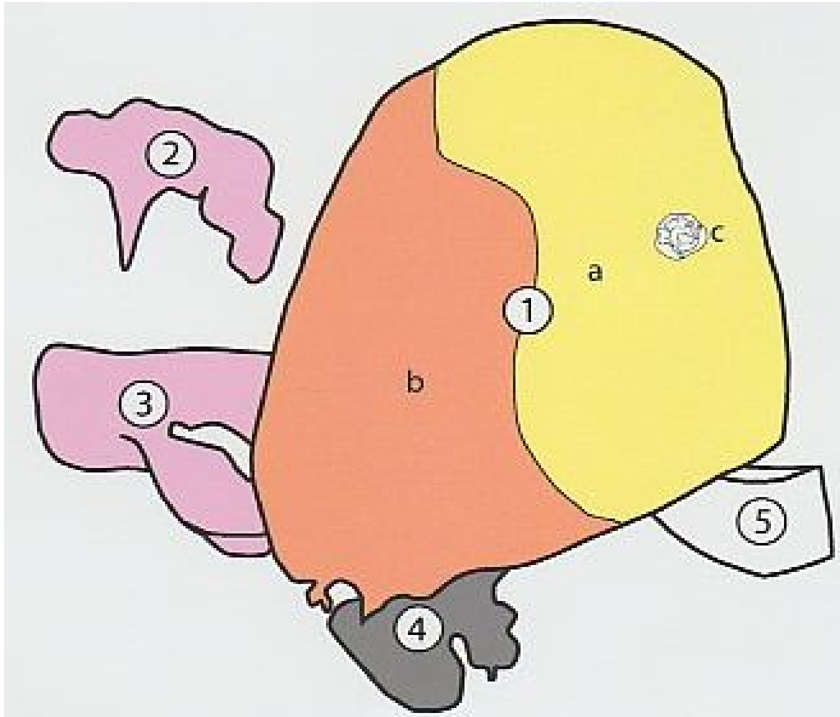

High-resolution SEM2 studies of e58 nearly particles

The two SEM2 Figure 10 high-resolution photographs (6000x) show respectively : 1/ In LFD, the e58 and nearly particles (with dimensions), and 2/ In CBS, the e58 and e55, e59, e60, e61, e62, e63 and e64 nearly particles. The lower Figure 11 spectrum shows that elemental analysis of e59 and e60 particles include barium and cadmium (with copper traces) components ; they indicate two particles of dyes (of light red yellow colour). The medium figure 11 spectrum indicates that the e62 particle is mainly constituted of calcium carbonate, that is of white colour and birefracts (see figures 2.1 and 2.2). The higher figure 11 spectrum shows that the e63 particle (with two sulphur and calcium peaks) is a particle of gypsum. The lower Figure 12 spectrum shows that e55particle is highly rich in lead. The upper figure 12 spectrum shows that e51 contains phosphorus and calcium as the main minor mineral peaks (with iron traces) ; it is a pluri-cellular microscopic marine algae (see the figure 3 photograph for more details concerning its morphology), with a tech (the algae substratum) relatively rich in calcium phosphate.

Mapping of the e58 region

Colour photographs of Figure 13 show EDX-mapping of elements C, O, P, Ca and Pb for e58 and other neighbouring particles. As expected, phosphorus and calcium are mainly distributed among e58 (there is also a small Ca amount in the calcium carbonate e62 particle). Concerning organic matter, carbon is mainly spread out in F4 and in e64, and oxygen in e58. The main lead density concerns the e55 particle, that contaminates F4 and e58.

Conclusions

Modern techniques of SEM-EDX analysis are very useful to study microscopy and chemical composition of human bones (Solari et al. , 2013). We have identified here a bone fragment, that corresponds to the e58 particle located in the Ec sub-area of the triangle. Elemental analysis shows that the e58 particle is mainly constituted of the P and Ca elements (calcium phosphate). The relative importance of the organic part (C and O) of the particle varies according to its location at the e58 surface. Minor chemical elements of the e58 spectra are silicium, magnesium and sodium. We obtain a similar elemental composition for an ancient human bone of another relic at the Christ ‘ time (Figure 14) : that of an authenticate bone of Ste Marie-Madeleine (Lucotte, 2016b); this spongy-bone sample is an osseous scale of a probably vertebrate corpus.

High resolution SEM electronic microscopy permit us to observe at least two different zones of the ultrastructure at the e58 surface : the main part (at the upper and the lower right) consists of fine micrograins (light to electrons in BSE) of calcium phosphate ; the rest (at the left lateral part and at the inferior basis) of the particle is mainly organized in elongated micro-reliefs. Part 1 (the granular part) consists of hydroxyapatite micrograins inserted into the osseous matrix, and part 2 (the fibrous part), relatively rich in organic matter, consists above all of elongated collagen microfilaments. We interprete part 1 as the really bone part of the e58 particle, part 2 representing its cartilaginous part. Figure 15 shows a schematic reconstitution (in colour) of the e58 particle, with its three sub-parts (the third one being the "heated"sub-part), and of the nearly neighbouring e particles. The e59 and e60 particles (in red) are dyes ; the e62 particle is the calcium carbonate ; the e63 particle is the gypsum, probably (see on the upper spectrum of figure 12 the relative – to carbon-fall in height of the oxygen peak) a plaster piece.Table 3 enumerates the characteristics of the e58 particle and all argumentations in favour to its osseous constitution. In our sense there is no doubts at all that the e58 particle is a bone/cartilage scale.

Table 3. Characteristics and indications about the osseous nature of the e58 particle.

1. Aspect : a little (10on 8.2 μm), ovaloid in form, flat scale.
2. Colour : yellow-white.
3. Thickness : with some thickness.
4. Composition : mainly constituted of calcium phosphate.
5. Ultrastructure : evidences of fine micrograins of hydroxyapatite, inserted into a protein matrix.

Why such an osseous remain on the surface of the triangle? We know (Lucotte and Thomasset, 2017) that this triangle is some part of a larger sticky tape that was applied to a blood area of the Face located just under the well-known blood spot of omega-form that flows on the front. This area is precisely located at the right eyebrow level, near the nose basis region. Several medical specialists have described the various injuries of the Man depicted on the TS (e.g. Zugibe, 2005). One of them concerns the nose : if a line is drawn following the bridge of the nose, starting from the horizontal level of the eyebrows and downwards , some displacement to the right of the distal part of this line is observed (Svensson, 2010); that can be diagnosed as a nose bone fracture. More recently, two groups of authors (Bevilacqua et al., 2014 ; Majorana et al., 2015) have confirmed the existence of this fracture of the nasal bone/cartilage. On the TS images of the Face –like that of the Enrie's photograph-the approaching of the tip of the nose to the upper lip forms a sort of "saddle nose", that is comparable to a fracture of the nasal cartilage (as a result of a blunt trauma). Otherwise the right eyebrow arcade seems notably swollen (that indicates another supplementary traumatism at this level). We consider that the presence of the bone/ cartilage particle e58 in the corresponding blood spot is a consequence of these various trauma.We have not here the formal proof that the osseous e58 particle is of human origin. But this bone remain adds some new hard material to that we published previously concerning red blood cells (Lucotte, 2015c), skin debris (Lucotte, 2016a) and one hair (Lucotte and Thomasset, 2017), originating from the Man whose Face image is imprinted on the Turin Shroud.

References

Bevilacqua M, Fanti G, D'Arienzo M, de Caro R. 2014. Do we really need new medical information about the Turin Shroud? Injury, International Journal Care Injuried **45** : 460-464.

Catanese JJ, Featherstone JDB, Keaveny TM. 1999. Characterization of the mechanical and ultrastructural properties of heat-treated cortical bone for the use as a bone substitute. Journal of Biomedical and Material Research **45** : 327-336.

Garcia Garduno MV, Dettmer Mendoza P, Moran Reyes A, Ramirez J, Reyes Gasga J. 2010. Study of mandibular necrosis due to bisphosphonates versus healthy bone by scanning electron microscopy and X-ray energy dispersive spectrometry. Acta Microscopica **19** : 100-104.

Joschek S, Nies B, Krotz R, Gofpferich A. 2000. Chemical and physiochemical characterization of porous hydroxyapatite ceramics made of natural bones. Biomaterials **21** : 1645-1658.

Lucotte G. 2012. Optical and chemical characteristics of the mineral particles found on the Face of the Turin Shroud. Scientific Research and Essays **7** : 2545-2553.

Lucotte G. 2015a. Exploration of the Face of the Turin Shroud. Linen fibers studied by SEM analysis. International Journal of Latest Research in Science and Technology **4** : 78-83.

Lucotte G. 2015b. Exploration of the Face of the Turin Shroud. Pollens studies by SEM analysis. Archaeological Discovery **3** : 158-178.

Lucotte G. 2015c. Red blood cells on the Turin Shroud. Jacobs Journal of Hematology **1** : 1-24.

Lucotte G. 2016a. Skin debris on the Face of the Turin Shroud : a SEM-EDX analysis. Archaeological Discovery **4** : 103-117.

Lucotte G. 2016b. The mitochondrial DNA mitotype of Sainte Marie-Madeleine. International Journal of Sciences **5** : 10-19.

Lucotte G., Thomasset T. (2017). Scanning electron microscopic characterization and elemental analysis of one hair located on the Face of the Turin Shroud. Archaeological Discovery **5** : 1-21.

Majorana A, Bardellini E, Gulino G, Conti G, Farronato G, Rodella L. 2015. The Turin Shroud face : the evidence of maxilla-facial trauma.Folia Morphologica **74** : 212-218.

Marion A, Lucotte G. 2006. Le Linceul de Turin et la Tunique d'Argenteuil. Presses de la Renaissance : Paris, France.

Miculescu F, Antoniac I, Ciocan LT, Miculescu M, Brânzei M, Ernuteanu A, Batalu D, Berbecaru A. 2011. Complex analysis on heat treated human compact bones. University Politechnia Bucharest Scientific Bulletin **73** : 203-212.

Riggi di Numana G. 1988. Rapporto Sindone 1978/1987. 3M Edizioni : Milano, Italy.

Solari A, Olivera D, Gordillo I, Bosch P, Fetter G, Lara VH, Novelo O. 2013. Cooked bones? Methods and practice for identifying bones treated at low temperature. International Journal of Osteoarchaeology. DOI : 10.1002/oa.2311.

Svensson N. 2010. Medical and forensic aspects of the Man depicted on the Turin Shroud. In Proccedings of the International Workshop on the Scientific Approach to the Archeiropoietos Images (p. 181-186). ENEA Frascati, Italy.

Zugibe F. 2005. The crucifixion of Jesus, a forensic inquiry. M Evans and Co. : New York, USA.